Contribution from the Department of Chemistry, State University of New York at Buffalo, Buffalo, New York 14214, and The Frank J. Seiler Research Laboratory, United States Air Force Academy, Colorado Springs, Colorado 80840

Studies of Titanium(IV) Chloride in a Strongly Lewis Acidic Molten Salt: Electrochemistry and Titanium NMR and Electronic Spectroscopy

R. T. Carlin,[†,‡] R. A. Osteryoung,*[,†] J. S. Wilkes,[§] and J. Rovang[§,∥]

Received November 7, 1989

The electrochemistry of titanium(IV) has been examined in acidic ($AlCl_3$-rich) compositions of the ambient-temperature molten salt, $AlCl_3$–1-ethyl-3-methylimidazolium chloride (ImCl). Titanium is reduced to Ti(III) and Ti(II) in two one-electron steps, both of which exhibit slow electron-transfer kinetics. The ^{49}Ti NMR spectra for $TiCl_4$ and $AlCl_3$-rich melts exhibit a resonance at −4 ppm (^{49}Ti = 0 ppm for neat $TiCl_4$). In basic (chloride-rich) melts, the ^{49}Ti resonance for $TiCl_6^{2-}$ is found at −237 ppm. In acidic melts, Ti(IV) is alkylated upon addition of $Me_3Al_2Cl_3$ and is slowly reduced to Ti(III). Combination of $TiCl_4$ and $Me_3Al_2Cl_3$ in an acidic melt is demonstrated to be a catalytic system for ethylene polymerization.

Introduction

The ambient-temperature molten salts derived from combining 1-ethyl-3-methylimidazolium chloride (ImCl) or *n*-butylpyridinium chloride (BupyCl) with $AlCl_3$ have been used extensively to study the electrochemistry of transition-metal chloro complexes.[1-3] When the $AlCl_3$:ImCl molar ratio is >1, the melt is termed acidic, and it contains the strongly Lewis acidic anion, $Al_2Cl_7^-$. When the $AlCl_3$:ImCl molar ratio is <1, the melt is termed basic, and it contains excess chloride anions, which complex strongly to transition-metal solutes. In both acidic and basic melts, the weakly ligating anion $AlCl_4^-$ accounts for the balance of the negative charge. Depending upon the composition of the melt, transition-metal solutes can display widely variable spectroscopic and electrochemical behavior as a consequence of differences in complexation.

Titanium(IV) has been investigated in the $AlCl_3$–BupyCl melt, but only melts of basic composition were employed.[4] In this melt, Ti(IV) is reduced to Ti(III) at −0.343 V versus an Al reference electrode. Both the Ti(IV) and the Ti(III) chloro complexes exist as the hexacoordinate species $TiCl_6^{2-}$ and $TiCl_6^{3-}$. A reduction wave for the oxochloro complex $TiOCl_4^{2-}$, formed from reaction of $TiCl_6^{2-}$ with oxide impurities in the melt, occurs at −0.77 V. Reduction of this oxochloro complex proceeds by an EC mechanism with the final reduction product being $TiCl_6^{3-}$.[4]

Cursory studies have been performed on Ti(IV) electrochemistry in ambient-temperature molten salts of acidic compositions.[3] Cyclic voltammetry of Ti(IV) in acidic $AlCl_3$–ImCl (molar ratio = 1.5:1.0) shows erratic behavior with no clearly defined voltammetric waves.[3] Yet, unpublished studies have shown that at a rotating disk electrode, Ti(II) can be oxidized in two one-electron steps to Ti(IV) in an acidic $AlCl_3$–ImCl melt at moderately elevated temperatures.[5]

In the higher temperature $AlCl_3$–NaCl system, Ti(II) is oxidized in two one-electron steps to Ti(IV).[6]

Titanium cannot be reduced to the metal in either the ambient-temperature melts or the $AlCl_3$–NaCl melts. High-temperature alkali-metal halide molten salts are required to achieve titanium deposition.[7,8]

Because of the lack of adequate and consistent information regarding the electrochemistry of Ti(IV) in the ambient-temperature acidic melts, we initiated an investigation into this area. In addition, since titanium has two NMR-active nuclei, ^{47}Ti and ^{49}Ti, we conducted titanium NMR studies in both acidic and basic melts.

Experimental Section

Titanium tetrachloride (99.9%, Aldrich) and bis(trimethylaluminum) trichloride, $Me_3Al_2Cl_3$ (Aldrich), were used as received. ImCl was synthesized and purified as previously described.[9] Melts were prepared by slowly combining sublimed $AlCl_3$ (Fluka) and ImCl with stirring.

All experiments were performed at ambient temperature under a purified He atmosphere in a Vacuum Atmospheres drybox.

Electrochemical experiments were carried out in a glass vessel fitted with a Teflon top through which three holes were bored to accommodate the working, reference, and counter electrodes. The Pt working electrode (area = 0.020 cm^2) consisted of a 1.6-mm-diameter Pt disk sealed in Kel-F. The glassy-carbon (GC) working electrode (area = 0.071 cm^2) consisted of a 3-mm-diameter GC disk sealed in Kel-F. Both working electrodes were purchased from Bioanalytical Systems. Aluminum wires immersed in acidic 1.5:1.0 melts and contained in separate fritted tubes served as reference and counter electrodes.

Since protons are reduced at a Pt electrode at ca. 0.8 V in an acidic melt,[10] it was necessary to remove protonic impurities utilizing a technique developed in this laboratory.[11] A modification of the published procedure comprised addition of $Me_3Al_2Cl_3$, instead of $EtAlCl_2$, with subsequent stirring of the melt for 1–2 h. The proton level was monitored with cyclic voltammetry at a Pt electrode. Due to the apparently slow reaction of the alkyl aluminum with low levels of protons, a small excess of alkylaluminum generally remained in the melt. As will be discussed, this excess alkylaluminum reacts with a portion of the Ti(IV), imparting a yellow color to the normally colorless melt.

Cyclic voltammetric (CV) experiments were performed with an electrochemical system composed of an EG&G PARC Model 173 potentiostat/galvanostat, an EG&G PARC Model 175 universal programmer, and a Houston Instrument Model 200 XY recorder. Staircase-cyclic, normal-pulse, and reverse-normal-pulse voltammetries were performed with an EG&G PARC Model 273 potentiostat/galvanostat controlled by a computer system similar to that described elsewhere.[12]

Titanium NMR spectra were obtained on a Bruker AC-300 spectrometer. A capillary filled with neat $TiCl_4$ and placed directly in the 10-mm sample tubes provided an external reference signal.

UV–vis spectra were obtained on a Hewlett-Packard Model 8452A diode-array spectrophotometer employing quartz cells with 1-mm path lengths.

[†] State University of New York at Buffalo.
[‡] Present address: Department of Chemistry, University of Alabama, Tuscaloosa, Alabama 35487.
[§] United States Air Force Academy.
[∥] Present address: Department of Chemistry, University of Cincinnati, Cincinnati, Ohio 45221.

(1) Osteryoung, R. A. Organic Chloroaluminate Ambient Temperature Molten Salts. In *Molten Salt Chemistry*; Mamantov, G., Marassi, R., Eds.; NATO ASI Series C; Reidel: Dordrecht, The Netherlands, 1987; Vol. 202, pp 329–364.
(2) Hussey, C. L. In *Advances in Molten Salt Chemistry*; Mamantov, G., Ed.; Elsevier: Amsterdam, 1983; Vol. 5, pp 185–229.
(3) Piersma, B. J.; Wilkes, J. S. Frank F. Seiler Research Laboratory Technical Report FJSRL-82-0004; USAF Academy: Colorado Springs, CO, 1982.
(4) Linga, H.; Stojek, Z.; Osteryoung, R. A. *J. Am. Chem. Soc.* **1981**, *103*, 3754.
(5) Gilbert, B. Unpublished results.
(6) Fung, K. W.; Mamantov, G. *J. Electroanal. Chem. Interfacial Electrochem.* **1972**, *35*, 27.
(7) Plambeck, J. A. *Encyclopedia of Electrochemistry of the Elements*; Bard, A. J., Ed.; Marcel Dekker: New York, 1976; Vol. X.
(8) Ferry, D. M.; Picard, G. S.; Tremillon, B. L. *J. Electrochem. Soc.* **1988**, *135*, 1443.
(9) Wilkes, J. S.; Levisky, J. A.; Wilson, R. A.; Hussey, C. L. *Inorg. Chem.* **1982**, *21*, 1263.
(10) Sahami, S.; Osteryoung, R. A. *Anal. Chem.* **1983**, *55*, 1970.
(11) Zawodzinski, T.; Carlin, R. T.; Osteryoung, R. A. *Anal. Chem.* **1987**, *59*, 2693.
(12) Brumleve, T. R.; O'Dea, J. J.; Osteryoung, R. A.; Osteryoung, J. *Anal. Chem.* **1981**, *53*, 702.

0020-1669/90/1329-3003$02.50/0

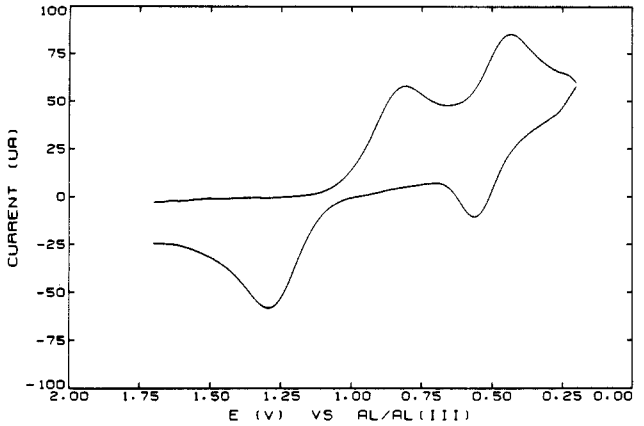

Figure 1. Staircase cyclic voltammogram for reduction of 40 mM Ti(IV) in 1.5:1.0 $AlCl_3$–ImCl molten salt at a Pt electrode. Scan rate = 250 mV s^{-1}; step height = 10 mV.

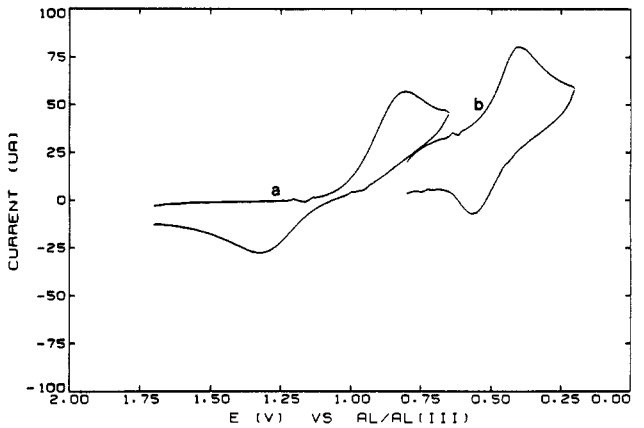

Figure 2. Staircase-cyclic voltammogram for the solution described in Figure 1, with (a) scan reversal following first reduction peak and (b) following hold at 0.8 V for 1 s at a Pt electrode. Scan rate = 250 mV s^{-1}; step height = 10 mV.

Results and Discussions

Electrochemistry. Several electrochemical techniques were used. The observations were complicated by the somewhat variable behavior of the Ti(IV) electrochemistry, which is influenced by numerous factors including electrode material, electrode history, melt history, and Ti(IV) concentration. Qualitatively, all the techniques confirmed the presence of the Ti(IV)/Ti(III) and Ti(III)/Ti(II) couples, and despite the variable behavior, it was possible to quantitatively analyze data in most cases.

Initially, staircase-cyclic voltammetry was employed to examine the titanium electrochemical couples. A staircase-cyclic voltammogram for 40 mM $TiCl_4$ in 1.5:1.0 $AlCl_3$–ImCl at Pt is shown in Figure 1. The melt was treated with $Me_3Al_2Cl_3$ to remove protonic impurities as discussed above. The two redox couples, Ti(IV)/Ti(III) and Ti(III)/Ti(II), are apparent. The Ti(III)/Ti(II) couple possesses a large peak potential separation with a cathodic peak potential, E_p^c, near 0.8 V and an anodic peak potential, E_p^a, at approximately 1.3 V. The Ti(III)/Ti(IV) couple demonstrates more reversible behavior with approximate E_p^c and E_p^a values of 0.4 and 0.55 V, respectively.

The two processes are also shown in Figure 2; in this case the Ti(III)/Ti(II) couple was examined following a potential hold of 1 s at 0.8 V. For hold times ≥20 s at 0.8 V, the working electrode becomes partially blocked by a brown film, presumably a Ti(III) species. At shorter times, this film is visually observed; however, it does not significantly degrade the working electrode's performance. The film can be removed by stepping the potential to +1.7 V or by physically wiping the electrode. Because the shape of the wave for the Ti(III)/Ti(II) couple resembles that expected for soluble species, the Ti(III) must have some solubility in the melt, and it is the soluble Ti(III) that is further reduced to Ti(II). The lack of reduction of the precipitated Ti(III) is confirmed by the fact that no Ti(III) reduction wave is observed when the potential is held at +0.8 V for 60 s, a sufficiently long time to completely block the electrode.

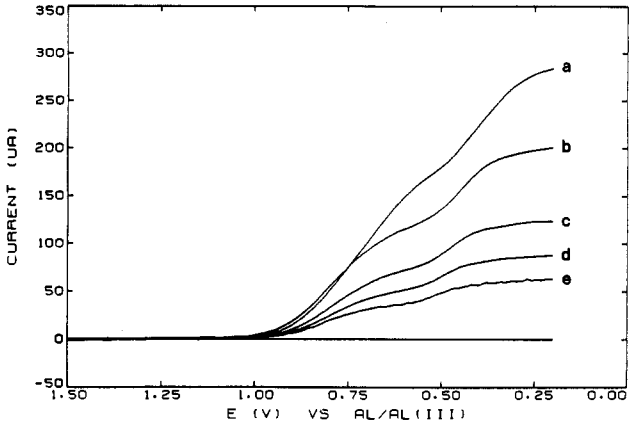

Figure 3. Normal-pulse voltammograms for 40 mM $TiCl_4$ in a 1.5:1.0 $AlCl_3$–ImCl melt at a Pt electrode. t_p (ms) = (a) 50, (b) 100, (c) 250, (d) 500, and (e) 1000.

Table I. Normal-Pulse Results for Reduction of Ti(IV) to Ti(III), Wave A, and for Subsequent Reduction of Ti(III) to Ti(II), Wave B (40 mM $TiCl_4$ in 1.5:1.0 $AlCl_3$–ImCl at a Pt Electrode)

	A		B		
t_p, ms	i_{NP}^c, μA	$E_{1/2}^c$, V	i_{NP}^c, μA	$E_{1/2}^c$, V	$i(A)/i(B)$
50	172	0.72	111	0.39	0.64
100	121	0.78	75	0.44	0.62
250	75	0.78	47	0.47	0.63
500	51	0.79	35	0.49	0.68
1000	36	0.81	26	0.50	0.72

Double-potential step chronocoulometry was performed at the Pt electrode to demonstrate formation and stripping of the Ti(III) film. Stepping the potential from +1.7 to +0.7 V and holding at this potential for 60 s resulted in passage of 658 μC of cathodic charge, while stepping back to +1.7 V and holding for 60 s resulted in passage of 477 μC of anodic charge. For completely soluble species, i.e. no reactant or product adsorption, the theoretical ratio of the charge passed for each step is given by

$$Q_d(t > \tau)/Q_d(\tau) = (t/\tau)^{1/2} - [(t/\tau) - 1]^{1/2} \qquad (1)$$

where Q_d is the charge from the diffusing species, t is the total time from the start of the experiment, and τ is the time of the first step only.[13] For equal step times ($t = 2\tau$) the theoretical charge ratio is calculated to be 0.414. For the Ti(IV)/Ti(III) couple studied here, the charge ratio of 0.72 indicates more product is recovered than expected; i.e., Ti(III) is deposited on the electrode surface, and it is oxidized from the surface in the reverse step. This is consistent with the visual observation that the film can be completely removed by holding the electrode at a potential positive to the Ti(IV)/Ti(III) couple.

Although we have not characterized the Ti(III) film, it is probably the β-$TiCl_3$ phase.[14] This phase is a brown solid prepared by low-temperature reduction of $TiCl_4$.[14]

A series of normal-phase voltammograms at Pt are shown in Figure 3 for 40 mM $TiCl_4$ in the 1.5:1.0 $AlCl_3$–ImCl melt. Between pulses, the potential was held at 1.7 V while the solution was stirred for 3 s followed by a 7-s wait to allow the solution to become quiescent. This treatment restores the initial Ti(IV) concentration at the electrode surface and removes any Ti(III) film. The reduction waves exhibit poorly resolved diffusion-limited current plateaus. Estimates of the diffusion-limited cathodic currents, i_{NP}^c, and of the half-wave potentials are summarized

(13) Bard, A. J.; Faulkner, L. R. *Electrochemical Methods*; Wiley: New York, 1980.
(14) Cotton, F. A.; Wilkinson, G. *Advanced Inorganic Chemistry*; Wiley-Interscience: New York, 1980; p 701.

Table II. Cyclic Voltammetric Parameters for Reduction of Ti(IV) to Ti(III), Wave A, and for Reduction of Ti(III) to Ti(II), Wave B (13.4 mM $TiCl_4$ in 1.5:1.0 $AlCl_3$–ImCl at a Pt electrode)[a]

scan rate, mV s^{-1}	E_p^c, V	i_p^c, μA	E_p^a, V	i_p^a, μA
		Wave A		
5	0.768	2.6 (37)[b]	1.315	0.7 (10)[b]
10	0.752	3.5 (34)	1.350	1.6 (16)
20	0.730	4.7 (33)	1.385	2.2 (15)
50	0.685	7.8 (35)	1.414	3.4 (15)
100	0.650	10.6 (33)	1.430	4.3 (14)
200	0.610	14.0 (31)	1.480	4.8 (10)
		Wave B		
10	0.460	1.7 (17)	0.562	1.7 (17)
20	0.445	2.4 (17)	0.572	2.3 (16)
50	0.437	3.1 (14)	0.592	2.5 (11)
100	0.425	4.8 (15)	0.607	3.6 (11)
200	0.407	6.9 (15)	0.625	4.5 (10)

[a] Potentials are ±5 mV. [b] Values in parentheses are $i_p v^{-1/2}$.

in Table I. The low limiting currents for the Ti(III)/Ti(II) reduction may be due to the film formation discussed above. To obtain a diffusion coefficient for Ti(IV), the Ti(IV)/Ti(III) reduction wave was analyzed by employing the Cottrell equation

$$i_{NP} = nFAC(D/\pi t_p)^{1/2} \quad (2)$$

in which n is the number of electrons transferred, F is the Faraday constant, A is the area of the electrode, D is the diffusion coefficient of the electroactive species, C is the bulk concentration of the electroactive species, and t_p is the pulse width.[15]

The slope of i_{NP}^c vs $t_p^{-1/2}$ for the first reduction yields a straight line from which a diffusion coefficient of 8.1×10^{-7} cm^2 s^{-1} (R = 0.999) is calculated for Ti(IV) in an acidic 1.5:1.0 $AlCl_3$:ImCl melt at 27 °C. Analysis of the sum of the two cathodic currents using n = 2 gives a diffusion coefficient of 5×10^{-7} cm^2 s^{-1} (R = 0.9998). However, due to possible Ti(III) precipitation onto the electrode surface and in solution, this lower value is probably erroneous. The higher value determined from the first cathodic wave is probably a good estimate, given the uncertainties in the limiting current; see Figure 3. The value of the Ti(IV) diffusion coefficient is that expected in these rather viscous melts; the absolute viscosity of a 1.5:1.0 $AlCl_3$–ImCl melt is 15 cP at 27 °C.[16] For comparison, Fe(III) has a diffusion coefficient of 9.3×10^{-7} cm^2 s^{-1} in acidic $AlCl_3$–ImCl at 30 °C.[17]

It is necessary to point out that other normal-pulse experiments performed at Pt and GC electrodes generally gave voltammograms in which the two reduction waves were less well resolved than those in Figure 3, and the ratios of the two diffusion-limited currents were <0.5. The performance of the Pt electrode appears to degrade with time, and as stated earlier, numerous experimental parameters may alter the quality of the data.

With an estimate of the Ti(IV) diffusion coefficient in hand, an effort was made to determine heterogeneous electron-transfer rate constants by using analog cyclic voltammetry. To minimize Ti(III) film formation on the electrode, a lower concentration, 13.4 mM, of Ti(IV) was employed. Results for analog cyclic voltammetry experiments are summarized in Tables II and III. At the Pt electrode the anodic and cathodic peak potentials for the Ti(IV)/Ti(III) couple are widely separated and shift 80–100 mV for a 10-fold increase in scan rate, and the value of $E_p - E_{p/2}$ for both the anodic and cathodic waves is >110 mV for all scan rates. These are traits generally ascribed to an irreversible electrochemical process.[13] At GC, the Ti(IV)/Ti(III) reduction wave was similar in shape to that at Pt, but the oxidation was sharper and resembled a stripping wave. Because the equilibrium potential of the Ti(IV)/Ti(III) couple is not known, it was not possible to calculate a heterogeneous rate constant for this couple; instead, it can only be stated that the couple appears to be electrochemically irreversible.

Table III. Cyclic Voltammetric Parameters for Reduction of Ti(IV) to Ti(III), Wave A, and for Reduction of Ti(III) to Ti(II), Wave B (13.4 mM $TiCl_4$ in 1.5:1.0 $AlCl_3$–ImCl at a GC Electrode)[a]

scan rate, mV s^{-1}	E_p^c, V	i_p^c, μA	E_p^a, V	i_p^a, μA
		Wave A		
20	0.825	12.8 (90)[b]	1.242	11.1 (78)[b]
50	0.830	20.8 (93)	1.249	16.2 (72)
100	0.825	30.1 (95)	1.255	21.5 (68)
200	0.810	42.0 (93)	1.260	25.0 (56)
500	0.783	60.0 (84)		
		Wave B		
5	0.476	2.2 (31)	0.551	3.9 (55)
10	0.465	3.6 (36)	0.556	5.1 (51)
20	0.460	5.9 (41)	0.562	6.2 (44)
50	0.451	8.7 (39)	0.572	9.8 (43)
100	0.443	14.0 (44)	0.580	13.0 (41)
200	0.430	19.5 (43)	0.590	18.8 (42)
500	0.405	20.5 (30)	0.607	15.5 (21)

[a] Potentials are ±5 mV. [b] Values in parentheses are $i_p v^{-1/2}$.

Table IV. Heterogeneous Electron-Transfer Rate Constants for Ti(III)/Ti(II) in 1.5:1.0 $AlCl_3$–ImCl

scan rate, mV s^{-1}	10^4k, cm s^{-1} at Pt	10^4k, cm s^{-1} at GC	scan rate, mV s^{-1}	10^4k, cm s^{-1} at Pt	10^4k, cm s^{-1} at GC
5		11	100	4.5	8.4
10	5.4	7.7	200	6.3	8.4
20	4.4	7.5	500		7.7
50	4.5	7.7			

At both electrodes, the Ti(III)/Ti(II) couple, which was examined following a 30-s hold at 0.6 V, demonstrates quasi-reversible behavior.[13] To test for blocking of the electrode, multiple consecutive scans were carried out on the Ti(IV)/Ti(III) couple. After the first two scans, the voltammograms reached the steady state, and subsequent scans showed no significant changes in the i_p and E_p values, indicating little or no blocking of the electrode. Only initial scans were used for the rate constant analysis. By use of the method of Nicholson, heterogeneous rate constants were determined for each scan rate at both Pt and GC electrode.[18] With this method, values for $E^{0\prime}$ are not needed since ΔE_p values are essentially independent of α, the transfer coefficient; heterogeneous rate constants are determined from ΔE_p values measured from scan reversal.[18] For the calculations, a diffusion coefficient of 8.1×10^{-7} cm^2 s^{-1} was assumed for both Ti(III) and Ti(II) species. Results are summarized in Table IV. The values calculated for the heterogeneous rate constant are consistent over the scan rates employed. The difference in the rate constants for Pt and GC may be due to actual properties of the two electrode materials, or they may be experimental artifacts. In any case the values are quite similar and are in the range normally assigned to quasi-reversible processes.[13]

As a check for the possibility of IR-drop contributions to the calculated rate constants, the reference electrode can be assumed to be infinitely far from the working electrode, allowing usage of the equation for a planar electrode

$$R_u = 1/(4\kappa r) \quad (3)$$

where R_u is the uncompensated resistance, κ is the specific conductivity, and r is the radius of the electrode.[19] For a κ value of 0.016 Ω^{-1} cm^{-1},[16] R_u is 195 and 105 Ω for the Pt and GC electrodes, respectively. Consequently, the IR-drop ranges from 0.3 to 1.3 mV at Pt and from 0.6 to 2 mV at GC. These values are negligible compared to the observed peak potential separations and will not affect the calculation of the rate constants.

(15) Parry, E. P.; Osteryoung, R. A. *Anal. Chem.* **1965**, *37*, 1654.
(16) Fannin, A. A., Jr.; Floreani, D. A.; King, L. A.; Sanders, J. S.; Piersma, B. J.; Stech, D. J.; Vaughn, R. L.; Wilkes, J. S.; Williams, J. L. *J. Phys. Chem.* **1984**, *88*, 2614.
(17) Lipsztajn, M.; Osteryoung, R. A. *Inorg. Chem.* **1985**, *24*, 716.
(18) Nicholson, R. S. *Anal. Chem.* **1965**, *37*, 1351.
(19) Newman, J. *J. Electrochem. Soc.* **1966**, *113*, 501.

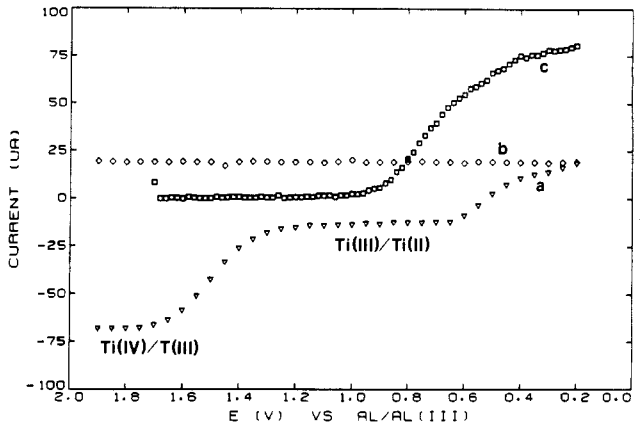

Figure 4. (a) Reverse-normal-pulse (RNP) voltammogram, (b) i_{DC} (see text), and (c) normal-pulse (NP) voltammogram for 13.4 mM $TiCl_4$ in 1.5:1.0 $AlCl_3$–ImCl at a Pt electrode. For RNP, τ = 2 s and t_p = 100 ms. For NP, t_p = 100 ms.

Table V. Reverse-Normal-Pulse Data for 13.4 mM Ti(IV) in 1.5:1.0 $AlCl_3$–ImCl at Pt

t_p, ms	τ, s	i_{DC}, μA	i_{RP}(III/II), μA	i_{RP}(IV/III), μA	i_{RP}(calcd),[b] μA
50	2	19.1	−25.0 (0.25)[a]	−101 (0.99)[a]	−102
100	2	18.9	−12.9 (0.20)	−68.1 (1.03)	−66.1
250	2	19.1	−2.8 (0.08)	−37.1 (1.03)	−36.0
500	2	19.2	−0.6 (0.05)	−22.3 (1.05)	−21.2
1000	2	19.0	0.0 (0.0)	−11.9 (1.05)	−11.4
100	1	25.0	−6.5 (0.12)	−57.2 (1.04)	−55.2
100	2	18.9	−12.9 (0.20)	−68.1 (1.03)	−66.1
100	5	12.1	−19.2 (0.26)	−71.0 (0.96)	−73.6
100	10	8.5	−23.0 (0.30)	−75.5 (0.99)	−76.5

[a] Values in parentheses are n_{RP}/n_{DC}. [b] $i_{RP} = n_{RP}i_{DC}/n_{DC}[(\tau/t_p)^{1/2} - (\tau/(\tau + t_p))^{1/2}]$; $n_{RP} = n_{DC} = 2$.

Finally, reverse-normal-pulse voltammetry (RNP) was performed in the 13 mM Ti(IV) solution to study the oxidation of Ti(II) back to Ti(III) and Ti(IV).[20] The pulse sequence consisted of initially stepping the potential from +1.8 to +0.2 V where it was held for times, τ, between 1 and 10 s to produce Ti(II) at the electrode. Then an analysis pulse, t_p, varied from 50 to 1000 ms, was applied at a more positive potential. Following the analysis pulse, the electrode potential was returned to +1.8 V, and the solution was stirred for 3 s and then allowed to become quiescent by waiting an additional 7 s. The treatment at +1.8 V completely removes any Ti(III) film from the electrode surface and restores the initial Ti(IV) concentration. This pulse sequence was repeated with the analysis pulse incrementally stepped to more positive potentials.

A representative reverse-normal-pulse voltammogram at Pt is shown in Figure 4, curve a. Two limiting current plateaus are closely seen in the RNP voltammogram: the first, labeled III/II, results from oxidation of Ti(II) to Ti(III), and the second, labeled IV/III, is due to final oxidation to Ti(IV). The constant-current line at 19 μA, curve b, is the current measured immediately prior to application of the analysis pulse and is referred to here as i_{DC}. Curve c is a NP (normal-pulse) voltammogram at Pt in the same solution. The two cathodic waves in the NP voltammogram are almost merged—further demonstrating the inconsistency of the electrochemical behavior in this system. In the RNP voltammogram, the irreversibility of the Ti(IV)/Ti(III) couple causes the wave for Ti(III) oxidation to occur ca. 0.7 V more positive than the Ti(IV) reduction wave in the NP experiment, thus separating it from the Ti(III)/Ti(II) couple. The Ti(III) oxidation wave in the RNP voltammogram is slightly positive of the Ti(II) reduction wave in the NP voltammogram as expected for a quasi-reversible couple.

(20) Osteryoung, J.; Kirowa-Eisner, E. *Anal. Chem.* **1980**, *52*, 62.

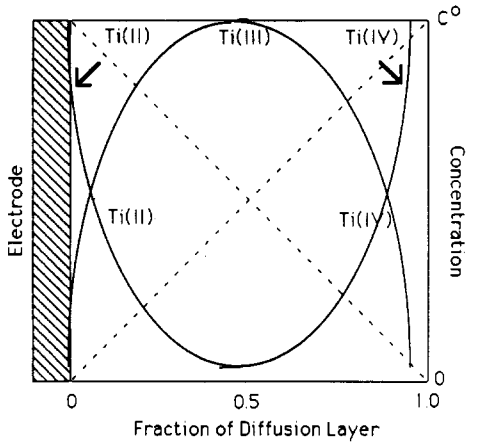

Figure 5. Drawing of the diffusion profile for Ti species during RNP experiments.

Results for numerous RNP voltammograms are listed in Table V. The reverse-phase current i_{RP}(III/II) is the diffusion-limited anodic current measured on the first plateau from zero current and corresponds to oxidation of Ti(II) to Ti(III), n = 1. The reverse-phase current i_{RP}(IV/III) is measured on the second plateau from zero current and is the total anodic current resulting from complete oxidation of Ti(II) to Ti(IV), n = 2. The half-wave potential for the Ti(II) oxidation to Ti(III) remains relatively constant at ca. 0.5 V for all RNP experiments. The half-wave potential for the other wave shifts from +1.38 V to t_p = 1000 ms to +1.54 V for t_p = 50 ms. The n_{RP}/n_{DC} values are calculated from eq 4 obtained by rearranging the published equation describing the diffusion-limited currents for a RNP experiment:[20]

$$n_{RP}/n_{DC} = (i_{RP}/i_{DC})[(\tau/t_p)^{1/2} - (\tau/(\tau + t_p))^{1/2}]^{-1} \quad (4)$$

An unusual trend is apparent from the n_{RP}/n_{DC} values. If all species are soluble and limiting currents are diffusion-controlled, the value of n_{DC} is 2, and the expected values for n_{RP}(III/II)/n_{DC} and n_{RP}(IV/III)/n_{DC} are 0.5 and 1, respectively. Interestingly, n_{RP}(IV/III)/n_{DC} has the expected value for all RNP experiments, but n_{RP}(III/II)/n_{DC} decreases with longer t_p and with shorter τ. The most probable explanation is that Ti(II) produced during the time τ at +0.2 V is oxidized back to Ti(III) by Ti(IV) diffusing from the bulk solution to the electrode, i.e. a reproportionation reaction as in eq 5.

$$Ti(IV) + Ti(II) \rightleftharpoons 2Ti(III) \quad (5)$$

Conceptually, the effect of this reproportionation reaction is to perturb the concentration profiles of the species near the electrode as represented by the drawing in Figure 5. During time τ, a diffusion layer is established in which, in the absence of chemical reactions, the concentration profiles for Ti(II) and Ti(IV) are represented by the dashed lines. No Ti(III) is present because the potential of the electrode is sufficiently negative to completely reduce Ti(IV) to Ti(II). With reaction of Ti(II) and Ti(IV) to produce Ti(III), the concentration profiles are altered as shown by the solid lines. Following establishment of this altered diffusion layer, the analysis pulse is applied. In a simplistic interpretation, the analysis pulse can be viewed as sampling the content of a species within the concentration profile at a specific distance from the electrode surface; long analysis pulses sample farther from the electrode surface than do short pulses. Therefore, very short t_p's will see only Ti(II), and the RNP voltammogram will display two plateaus of equal height. As t_p is made longer, the analysis pulse will see increasing amounts of Ti(III) relative to Ti(II), and the ratio i_{RP}(III/II):i_{RP}(IV/III) will decrease, eventually going to zero when t_p is sufficiently long. Finally, with longer τ, the diffusion layer is thickner, and longer analysis pulses are needed to probe the same relative distance from the electrode surface; i.e., the ratio of t_p to τ determines the quantity of Ti(III) observed in the RNP voltammogram. This simplified view of the perturbation of the concentration profiles requires a more detailed

Table VI. Comparison of Total NP and RNP Currents for Reduction of Ti(IV) to Ti(II), $n = 2$ (13.4 mM $TiCl_4$ in 1.5:1.0 $AlCl_3$–ImCl at 0.02 cm^2 Pt) ($\tau = 2$ s)

t_p, ms	$f(t_p,\tau)$, $s^{-1/2}$	i_{NP}, μA	$i_{RNP} + i_{DC}$, μA	ratio[a]
50	4.48	114	120	0.95
100	3.18	81	87	0.94
250	2.04	51	53	0.93
500	1.49	36	42	0.91
1000	1.13	26	31	0.95

[a] $i_{NP}t_p^{1/2}[f(t_p,\tau)]/(i_{RNP} + i_{DC})$.

analysis before the observed changes can be quantitated, and one is in progress.[21]

With appropriate substitution and rearrangements, eqs 2 and 4 can be used to show that the sum of i_{DC} and i_{RNP} is given by

$$i_{DC} + i_{RNP} = FAC(D/\pi)^{1/2}[n_{RNP}/t_p^{1/2} + n_{RNP}/\tau^{1/2} + n_{DC}/(t_p + \tau)^{1/2}] \quad (6)$$

When $n_{DC} = n_{RNP}$, eq 6 can be expressed as

$$i_{DC} + i_{RNP} = i_{NP}t_p^{1/2}f(\tau,t_p) \quad (6')$$

where

$$f(\tau,t_p) = t_p^{-1/2} + \tau^{-1/2} + (t_p + \tau)^{-1/2} \quad (7)$$

It should be noted that eq 6 simplifies to $i_{DC} + i_{RNP} = i_{NP}$ for $t_p \ll \tau$ and $n_{DC} = n_{RNP}$. A comparison of total RNP and NP currents ($n = 2$) obtained for 13.4 mM Ti(IV) is presented in Table VI.

Plotting $i_{DC} + i_{RNP}$ vs $f(\tau,t_p)$, whose slope should be $nFAC(D/\pi)^{1/2}$, provides a means for calculating diffusion coefficients from RNP data. Diffusion coefficients for Ti(IV) calculated from the total currents for $n = 2$, from RNP (eq 6′) and NP (eq 2) are 8.2×10^{-7} ($R = 0.9998$) and 7.5×10^{-7} ($R = 0.9999$) cm^2 s^{-1}, respectively. These values are in good agreement with the value of 8.1×10^{-7} cm^2 s^{-1} determined above from the first reduction wave for 40 mM Ti(IV). However, for reasons discussed earlier, the value determined from the NP data for $n = 2$ may be lower than the true value; therefore, the D value for Ti(IV) is taken as the average of the two higher values, i.e., 8.2×10^{-7} cm^2 s^{-1}.

The measurement of i_{DC} prior to the analysis pulse has advantages over the method employed in ref 20 where i_{DC} is measured following time ($\tau + t_p$). Although in ref 20 the mathematics are somewhat simplified, and the sum $i_{DC} + i_{RNP}$ is equal to i_{NP} when $n_{DC} = n_{RNP}$, a difficulty arises when it is not possible to observe a well-defined current plateau from which to determine i_{DC}. This is the case for the RNP voltammogram in Figure 4. In the measurement method employed here, i_{DC} is a constant measured during the entire RNP experiment and so can be accurately determined as seen in Figure 4b. Additionally, if i_{DC} does not remain constant during the course of the experiment, this may be an indication of electrode fouling or of insufficient solution stirring between pulse sequences.

Titanium NMR. Titanium NMR spectra were obtained on 0.5 M $TiCl_4$ in melts of various compositions. Titanium NMR spectra are unusual because the resonance frequencies of two isotopes are nearly the same (16.917 MHz and 16.912 MHz for ^{47}Ti and ^{49}Ti respectively) and the natural abundances are similar. Thus one can observe resonances from both isotopes in the same spectrum. The chemical shifts, δ, of the ^{49}Ti nucleus and the peak widths at half-height, $W_{1/2}$, are reported in Table VII for basic and acidic melts, and representative spectra are shown in Figure 6. The two resonances from neat $TiCl_4$ (external reference contained in a capillary) are labeled appropriately with the ^{49}Ti resonance set to 0 ppm. In acidic melts, the ^{49}Ti resonance is a sharp peak at −4 ppm, whereas the ^{47}Ti resonance is not clearly observed, but

Table VII. ^{49}Ti NMR Chemical Shifts, δ, and Peak Widths at Half-Height, $W_{1/2}$, for $TiCl_4$ in $AlCl_3$–ImCl Melts of Different Compositions

$AlCl_3$:ImCl	$\delta(^{49}Ti)$,[a] ppm	$W_{1/2}$, Hz	$AlCl_3$:ImCl	$\delta(^{49}Ti)$,[a] ppm	$W_{1/2}$, Hz
2.0:1.0	−4	58	1.0:1.0	−9	111
1.5:1.0	−4	53	0.9:1.0	−238	139
1.1:1.0	−5	67	0.8:1.0	−237	142

[a] Spectra are referenced to neat $TiCl_4$, $\delta(^{49}Ti) = 0$ ppm.

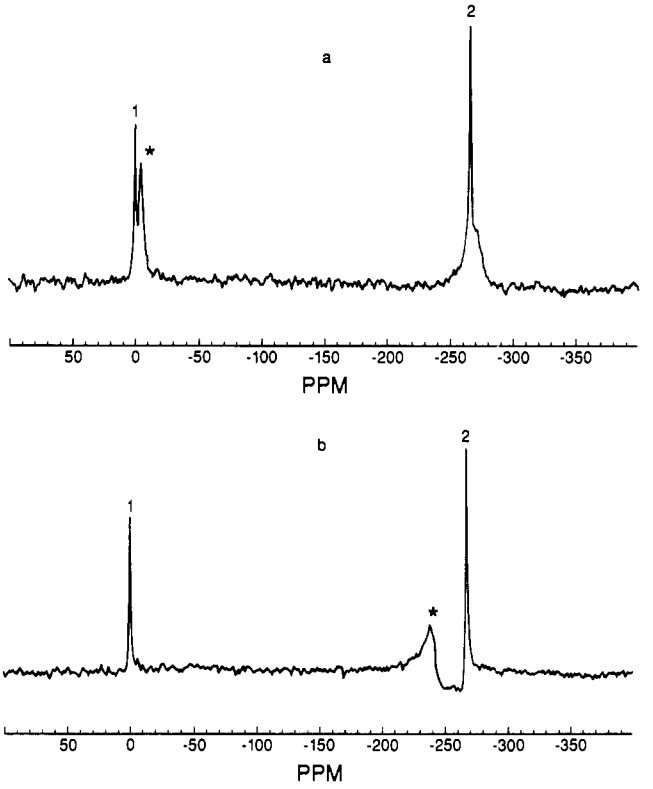

Figure 6. $^{47,49}Ti$ NMR spectra for 0.5 M $TiCl_4$ in (a) 1.5:1.0 and (b) 0.8:1.0 melts. Resonances for ^{49}Ti resulting from $TiCl_4$ dissolved in the melts are labeled with an asterisk. ^{49}Ti and ^{47}Ti resonances for the $TiCl_4$ external reference are labeled 1 and 2, respectively.

it may account for the shoulder on the high-field side of the ^{47}Ti reference signal. In basic melts, the ^{49}Ti resonance is a broad peak located at −237 ppm, but no ^{47}Ti resonance could be found at higher fields.

The ^{49}Ti chemical shift in acidic melts indicates the Ti(IV) complexation is akin to that in neat $TiCl_4$. It is reasonable to hypothesize that Ti(IV) in the acidic melt exists as $TiCl_4$ and that weak complexation with $Al_2Cl_7^-$ may occur. This is borne out by the UV–vis results (vide infra). The Ti NMR spectrum in the basic melt is the first reported for $TiCl_6^{2-}$. Previous efforts to study $TiCl_6^{2-}$ salts have been unsuccessful due to degradation of the anion to $TiCl_4$ in the organic solvents employed.[22] The shift to high field in going from $TiCl_4$ to $TiCl_6^{2-}$ is in the same direction as that reported for the bromide analogues $TiBr_4$ ($\delta = 482.9$) and $TiBr_6^{2-}$ ($\delta = 8.2$).[22]

The differences in the line widths of the ^{49}Ti resonances and the difficulties in observing the ^{47}Ti resonances can be understood from the equation describing the peak width at half-height for quadrapolar nuclei

$$W_{1/2} = (3\pi/10)[(2I + 3)/I^2(2I - 1)](1 + n^2/3)(e^2qQ/h)^2\tau_c \quad (8)$$

where I is the nuclear spin ($I = {}^5/_2$ for ^{47}Ti; $I = {}^7/_2$ for ^{49}Ti), Q is the nuclear electric quadrupole moment ($eQ = 0.29 \times 10^{-28}$

(21) Karpinski, Z.; Park, S-G.; Osteryoung, R. To be submitted for publication.

(22) Hao, N.; Sayer, B. G.; Denes, G.; Bickley, D. G.; Detellier, C.; McGlinchey, M. J. *J. Magn. Reson.* **1982**, *50*, 50.

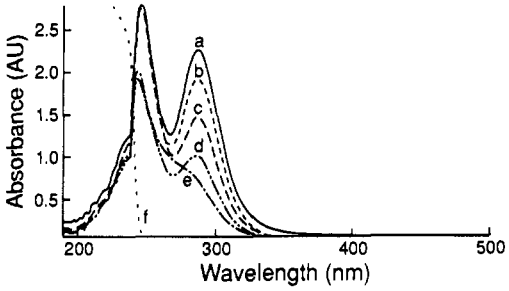

Figure 7. UV-visible spectra for 3 mM $TiCl_4$ in a 1.5:1.0 melt with increasing concentration of $Me_3Al_2Cl_3$. Me:Ti molar ratio = (a) 0, (b) 30, (c) 90, (d) 90 after 4 h, (e) >200 after several hours, and (f) melt cutoff.

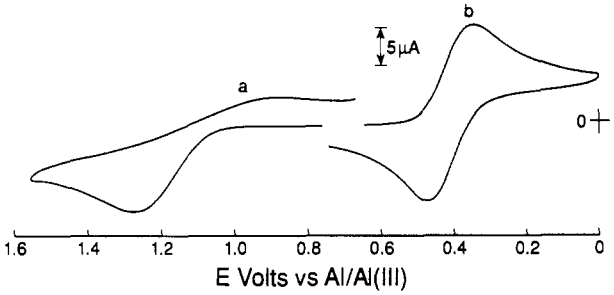

Figure 8. Cyclic voltammogram, (a) anodic and (b) cathodic scans, of 13.4 mM $TiCl_4$ in a 1.5:1.0 $AlCl_3$–ImCl melt following reaction for 12 h with excess $Me_3Al_2Cl_3$-GC electrode. Scan rate = 50 mV s^{-1}.

m^2 for ^{47}Ti; $eQ = 0.24 \times 10^{-28}$ m^2 for ^{49}Ti), eq is the field gradient, n is the asymmetric parameter describing the deviation from cylindrical symmetry, and τ_c is the correlation time characterizing the fluctuation of the electric field.[23] Substitution of the appropriate quantities into eq 8 reveals that the ^{49}Ti resonance half-width is expected to be 3.43 times smaller than the ^{47}Ti resonance. Therefore, despite the higher natural abundance of ^{47}Ti (7.28%) versus ^{49}Ti (5.51%), the ^{49}Ti resonance is more pronounced. Also, the 2–3 times higher viscosities of the basic melts versus acidic melts will result in longer values of τ_c for solutes in basic melts.[16] Consequently, $W_{1/2}$ values are larger in basic melts as seen in Table VII. The combination of these line-broadening effects accounts for the inability to observe any signal for ^{47}Ti in basic melts.

In melts near the neutral composition ($AlCl_3$:ImCl molar ratio = 1.0:1.0), the ^{49}Ti resonance begins to broaden and shift to slightly higher fields. A useful feature of the chloroaluminate melts is the ability to adjust the amount of free chloride (i.e., not complexed with Al) relative to a solute metal ion, which we express as the Cl:Ti molar ratio. A series of melts containing 0.5 M $TiCl_4$ were made in which the Cl:Ti molar ratio was increased from 0 (a neutral melt) to 3 (a chloride-rich melt) with the hope of observing a gradual shift in the ^{49}Ti resonance. A ^{49}Ti resonance was observed at −20 ppm ($W_{1/2}$ = 288 Hz) in the neutral melt but vanished in melts with 0 < Cl:Ti < 2. The resonance again appeared at −237 ppm in the melt with Cl:Ti = 3. These results are explained by the fact that Ti(IV) forms anions of formulas $TiCl_5^-$ and $Ti_2Cl_9^-$ in dichloromethane solution, and the equilibrium distribution of these two anions is determined by the Cl:Ti molar ratio.[24] The same anions are probably formed in melts where insufficient chloride anions are available to form the hexachloro Ti complex. Because these chloride-deficient anions are less symmetric than $TiCl_4$ and $TiCl_6^{2-}$ and are rapidly interconverted, they will be very difficult to observe with Ti NMR. In basic melts with high chloride anion concentrations, these Ti anions are fully converted to $TiCl_6^{2-}$, a symmetric, and therefore, NMR observable molecule. Also, the broadening and upfield shifts observed for the neutral melt and the 1.1:1.0 melt may be explained by $TiCl_4$ abstracting chloride from $AlCl_4^-$, giving rise to a small fraction of the chloride-deficient Ti anions.

It is important to point out that in Table VII, the 0.9:1.0 melt has a Cl:Ti molar ratio of only 1:1, yet a ^{49}Ti resonance is observed. This is contrary to the study just discussed in which no ^{49}Ti resonance was observed for solutions with Cl:Ti < 2. We can state with confidence only that the ^{49}Ti resonance for $TiCl_6^{2-}$ is observed in melts with sufficiently high concentrations of chloride anions to avoid forming these intermediate Ti anions. At this time, we are not certain of all the experimental parameters, e.g. Cl:Ti molar ratio, temperature, and sample history, which influence the ability to observe Ti NMR signals in the melts.

A final noteworthy point is that, in basic melts, a pale yellow precipitate often formed in the NMR tubes after several hours. This precipitate may be Im_2TiCl_6, although it was not characterized.

UV-vis Spectroscopy. The UV-vis spectra for 3 mM $TiCl_4$ in 1.5:1.0 $AlCl_3$–ImCl is shown in Figure 7. The absorption at 290 nm (ϵ = 8300 L mol^{-1} cm^{-1}) is the same reported for $TiCl_4$ in CCl_4,[25] validating the hypothesis, based on the NMR spectrum, that Ti(IV) exists as $TiCl_4$ in acidic melts. The absorption at 250 nm, which was not reported in ref 25, may be an instrumental artifact since it is near the 245 nm cutoff for the melt. We have found that background subtraction near the solvent cutoff can often give a false peak.

In the gas phase, $TiCl_4$ displays two absorptions at 281 nm (ϵ = 6900 L mol^{-1} cm^{-1}) and 232 nm (ϵ = 9000 L mol^{-1} cm^{-1}) corresponding to the ligand-to-metal charge-transfer transitions $(t_1)^6 \rightarrow (t_1)^5(2e)^1$ and $(t_1)^6 \rightarrow (t_5)^1(3t_2)^1$, respectively.[26] We tentatively assign the absorptions at 290 nm to the lower energy charge-transfer band. The second absorption occurs beyond the melt cutoff.

Addition of $Me_3Al_2Cl_3$ to 3 mM $TiCl_4$ in 1.5:1.0 $AlCl_3$–ImCl produces a yellow coloration of the melt and alters the absorption spectrum as shown in Figure 7, parts b (Me:Ti molar ratio = 30:1) and c (Me:Ti molar ratio = 90:1), where [Me] = 3[added $Me_3N_2Cl_3$]. The absorption at 290 nm decreases significantly with increasing $Me_3Al_2Cl_3$, while the 250-nm absorption remains unchanged, in accord with it not being a true $TiCl_4$ absorption band. Closer examination of the absorption spectra shows that the yellow color results from a weak tailing of the absorption spectrum into the visible range; no specific absorption in the visible region is apparent.

The changes in the spectra with $Me_3Al_2Cl_3$ addition are due to formation of a titanium alkyl. In the acid melt, the methyl group is in rapid exchange with $TiCl_4$ and the aluminum chlorides. Because of the high concentration of aluminum chlorides in the melt, it is necessary to add a large excess of $Me_3Al_2Cl_3$ to produce significant quantities of the titanium alkyl, undoubtably $TiCl_3Me$.

After 4 h, the absorption spectrum of the 90:1 Me:Ti solution was further changed as revealed in Figure 7d. The 290 nm band and the absorption at lower wavelength are both decreased as a result of decomposition (alkyl reduction) of the Ti(IV) alkyl to Ti(III). This decomposition has been well documented.[25,27] With a large excess of $Me_3Al_2Cl_3$ and after sufficient time, Figure 7e, the absorption at 290 nm disappears. After all the Ti(IV) is reduced, the melt is again colorless. With higher initial concentrations of $TiCl_4$, the alkyl reduction produced a brown precipitate, assumed to be β-$TiCl_3$.

To confirm that Ti(III) is the product of the alkyl reduction, a large excess of $Me_3Al_2Cl_3$ was added to the 1.5:1.0 melt containing 13.4 mM $TiCl_4$, and the components were allowed to react for 12 h. The resulting solution was colorless but displayed a faint brown cloudiness. The open circuit potential, 0.54 V, at a GC electrode, fell between the potentials of the two Ti couples. Cathodic and anodic scans from the open circuit potential clearly

(23) McGlinchey, M. J.; Bickley, D. G. *Polyhedron* **1985**, *4*, 1147.
(24) Creaser, C. S.; Creighton, J. A. *J. Chem. Soc., Dalton Trans.* **1975**, 1402.
(25) Behar, D.; Feilchenfeld, H. *J. Organomet. Chem.* **1965**, *4*, 278.
(26) Clark, R. J. H. *The Chemistry of Titanium and Vanadium*; Elsevier: Amsterdam, 1968; p 170.
(27) Beerman, C.; Bestian, H. *Angew. Chem.* **1959**, *71*, 618.

show the presence of only one Ti—i.e., Ti(III) species (Figure 8) confirming the complete conversion of Ti(IV) to Ti(III). Also, this affirms the statement made earlier that Ti(III) is soluble to some extent in the acidic melt.

Ethylene Polymerization. A logical extension of the Ti chemistry in these melts is to test for catalytic olefin polymerization. To this end, 0.5 g of $AlEtCl_2$ and 0.5 g of $TiCl_4$ were combined in 7.2 g of 1.1:1.0 $AlCl_3$–ImCl, resulting in the immediate production of a deep red solution. Bubbling ethylene into the melt at 1 atm induced the formation of a brown-green cloudiness. After several minutes of ethylene bubbling, the reaction was quenched with MeOH. Flakes of polyethylene were seen floating in the resulting clear MeOH solution. The polyethylene flakes (mp: 120–130 °C) were isolated via centrifugation. Although the yield of polyethylene was too low to quantitate, it is significant that the ambient-temperature molten salt can serve as a medium for catalytic polyethylene production. Higher yields of polyethylene have been achieved in acidic melts employing the homogeneous catalyst system: Cp_2TiCl_2/alkylaluminums.[28]

Conclusions

The $AlCl_3$–ImCl molten salt offers a unique medium for the examination of metal halides. It is an aprotic solvent that allows examination of the electrochemistry and spectroscopic properties of chloro complexes without coordination sphere changes often induced in organic solvents. Also, because it is used at ambient temperatures, it is possible to carry out organometallic reactions, e.g. metal alkylations, in the melts.

Acknowledgment. This work was supported by the Air Force Office of Scientific Research. We thank Dr. Janet Morrow for use of her spectroscopic equipment.

(28) Carlin, R. T.; Wilkes, J. S. To be submitted for publication.

Contribution from the Department of Chemistry, Wayne State University, Detroit, Michigan 48202

Tetranuclear Complexes of 1,3,5,9,11,13-Hexaketonates. 2. Synthesis and Electrochemistry of a Series of Heterotetranuclear Complexes, Bis{1,1′-(1,3-phenylene)bis[7-methyl-1,3,5-octanetrionato(4−)]}hexakis(pyridine)bis[dioxouranium(VI)]dimetal(II), $M_2(UO_2)_2(MOB)_2(py)_6$

R. L. Lintvedt,* W. E. Lynch, and J. K. Zehetmair

Received July 24, 1989

A series of heterotetranuclear complexes was prepared by using a 1,3,5,9,11,13-hexaketone ligand. The specific ligand used in this study contains two 1,3,5-triketone groups substituted at the meta positions of a benzene ring. Neutral complexes are formed by binding four dicationic metal species to two tetraanionic ligands. The resulting tetranuclear complexes contain two binuclear moities separated by about 7 Å. A series of complexes with two uranyl ions and two metal ions, M^{2+}, per molecule was prepared. Reaction of the ligand with UO_2^{2+} results in the selective coordination of the uranium to the "outside" (1,3 and 11,13) coordination sites of the hexaketonates. As a result, the UO_2^{2+} ions assemble the ligands so that the "interior" (3,5 and 9,11) coordination sites are available for binding the divalent metal ions M^{2+}. The electrochemical properties of the resulting $M_2(UO_2)_2(L)_2$ complexes were investigated by cyclic voltammetry, chronoamperometry, and controlled-potential electrolysis. The nature of the multielectron-transfer processes observed is discussed on the basis of the results of these experiments.

Introduction

Cooperative interactions between metal ions in polynuclear complexes continue to be a subject of considerable interest. An important part of this subject is the interactions between different metal ions in heteropolynuclear complexes. A difficulty that arises immediately when one attempts to address this problem is systematically designing and synthesizing pure compounds. Initially, we developed a strategy[1] that depends upon (1) using binucleating ligands with two different coordination environments, (2) selectively binding one metal ion to one of the sites and characterizing the mononuclear precursor, and (3) adding to the precursor complex a different metal ion that binds to the second site. This approach obviously is only applicable with unsymmetric ligands that have a significant sites selectivity for the metal ions of interest.

Another synthetic approach has been developed that is applicable to symmetric polynucleating ligands.[2-4] This involves preparing a mononuclear precursor complex in which the first metal ion assembles the ligands in a manner that facilitates the incorporation of the second, different metal ion. The UO_2^{2+} ion is very well suited to this approach because of its strong tendency to bind a fifth equatorial ligand. The resulting geometry forces a "cis" arrangement of the principal equatorial ligand and positions them to bind a second metal ion. This is shown in Figure 1 for the mononuclear UO_2^{2+} complex of 1,5-diphenyl-1,3,5-pentanetrionate, $UO_2(HDBA)_2(CH_3OH)$.[2] This precursor complex was used to prepare a series of heterobinuclear compounds containing a symmetric triketonate ligand.[3]

The same approach has been used to prepare heterotrinuclear complexes of a symmetric *tetra*ketone, 1,7-diphenyl-1,3,5,7-heptanetetraone (H_3DBAA).[4] In this case, two UO_2^{2+} ions preferentially bind to the terminal coordination sites (1,3 and 5,7) because of the stereochemical requirements of the fifth equatorial ligands. The central position (3,5) is available for binding a transition-metal ion. The structures of four compounds with the general formula $M(UO_2)_2(DBAA)_2(py)_4$ where M = Ni(II), Co(II), Fe(II), and Mn(II) were determined.[4] All are isomorphous. The structure is shown in Figure 2.

The electrochemistry of trinuclear $M(UO_2)_2(DBAA)_2(py)_4$ complexes showed very interesting patterns in which there is obvious communication between the U centers. The strength of the interaction between the uranium centers is sensitive to the identity of the M(II) metal ion and increases in the order Fe < Co < Ni < Cu < Zn. The present study was undertaken to investigate further the nature of the interactions in heteronuclear complexes containing the uranyl ion.

Experimental Section

I. Ligand Synthesis. A 1,3,7,9-tetraketone, 1,1′-(1,3-phenylene)bis-(4,4-dimethyl-1,3-pentanedione), abbreviated H_2DPB, was prepared by condensing dimethyl isophthalate and 3,3-dimethyl-2-butanone in THF with NaH. The product was recrystallized from methanol. Anal. Calcd for $C_{20}H_{26}O_4$: C, 72.69; H, 7.31. Found: C, 71.98; H, 7.26. Mp: 100 °C.

(1) Tomlonovic, B. K.; Hough, R. L.; Glick, M. D.; Lintvedt, R. L. *J. Am. Chem. Soc.* **1975**, *97*, 2925.
(2) Lintvedt, R. L.; Heeg, M. J.; Ahmad, N.; Glick, M. D. *Inorg. Chem.* **1982**, *21*, 2350.
(3) Lintvedt, R. L.; Ahmad, N. *Inorg. Chem.* **1982**, *21*, 2356.
(4) Lintvedt, R. L.; Schoenfelner, B. A.; Ciccarelli, C.; Glick, M. D. *Inorg. Chem.* **1984**, *23*, 2867.

0020-1669/90/1329-3009$02.50/0